A Fast Procedure for Computations of Acoustic Fields Given by Retarded-Potential Integrals

Florent Margnat

A fast procedure for the computation of acoustic fields given by retarded-potential integrals

Florent Margnat*

Arts et Metiers ParisTech, DynFluid Laboratory, 151 bd de l'Hopital, 75013 Paris, France

An optimized procedure for the computation of acoustic fields given by retarded-time intgrals is provided. It is written in the time-domain and for fixed sources. It is devoted to applications in which there is a large amount of source data. Thus, as many observer points are required to build the acoustic image, the resulting number of source-observer pair may cause an issue in accessing to the source-observer distance, if this quantity can not be stored in a global variable. The algorithm is validated through comparisons with reference data in the case of a simple harmonic source and in the case of the aerodynamic noise generated by the cylinder flow. The extension to the propagation in a moving medium is also presented, with the implementation of the convected Green function.

I. Introduction

Flow-generated acoustic fields are often predicted by computing retarded-potential integrals which appear in the formalism of aeroacoustic analogies or wave extrapolation methods. Such procedures return the acoustic emission of unsteady flows by two steps: firstly, the flow is simulated, giving access to source quantities (or to acoustic quantities on the control surface in the case of a wave extrapolation method); secondly, those quantities are propagated until observer/listener locations. This avoids the computation of the flow equation over a large domain including both the flow region and the acoustic region, which requires a carefull choice of numerical schemes and boundary conditions. Moreover, thanks to a source modelisation and propagation, access is given to the noise generated by flows simulated using CFD methods that are not able to generate (e. g. the incompressible assumption) or propagate (e. g. dissipative schemes) acoustic waves. Finally, if source quantities can be stored, the acoustic computation becomes a post-treatment, so it can be tested, optimised, independantly from the flow computation. Beside, the same acoustic tool can apply to source data from different CFD tools. For that reasons, in the field of computational aeroacoustics, hybrid prediction methods based on acoustic integrals stand as a current topic next to direct noise computation methods (see the review papers by Colonius & Lele [1] and Wang *et al.* [2]).

In the present contribution, the numerical implementation of a retarded-potential integral is adressed in the time-domain. An optimised method is provided for the computation of the acoustic quantity on an observer grid in order to build an acoustic *picture* - field. It is very useful when large size source data are considered, thus involving a large amount of source-observer distances which can not be stored in a global variable. It keeps the advanced time principle, which allows an acoustic prediction parallely to the flow simulation and an easy connection with usual CFD tools. Only fixed source domains are considered, however moving domains may be concerned by the specific technic presented hereafter.

The paper is organized as follows: first, the general formulation of the problem is presented. Then the principle of the optimized procedure is described, with an illustration of the CPU-time reduction that can be expected. The validation of the algorithm is performed through the case of a monopole radiating in a 2D medium. The algorithm is then extended to take into account a propagation in an uniformly moving medium, with the help of the convected Green function. Finally, an application example is provided with the noise radiated by the flow over a circular cylinder.

* Assistant Professor, Arts et Metiers ParisTech, DynFluid, Paris, France.

II. Principle of the procedure

A. Problem formulation

A general form of aeroacoustic integrals can be written, considering a source quantity S to be integrated over a source domain $\mathcal{D}$ in order to compute the acoustic quantity, pressure, at an observer position $\mathbf{x}$ and time t_a, as:

$$p_a(\mathbf{x}, t_a) = \frac{1}{4pi} \int_{\mathcal{D}} S\left(\mathbf{y}, t_a - \frac{|\mathbf{x}-\mathbf{y}|}{c_0}\right) \frac{d\mathbf{y}}{|\mathbf{x}-\mathbf{y}|} \tag{1}$$

where $\mathbf{y}$ denotes the position over the source domain and c_0 is the ambient sound speed. Such expression is usually called a retarded potential integral, since, unless the source is compact, the propagation distance deviation between two source points implies their respective contributions must be collected at different emission times in order to reach the observer point at the same time. Formally, it can stand for integrals to be handled at computing, e. g., the solution of Lighthill's [3] or Howe's equations in free-field, the volumic or surfacic terms appearing in Curle's analogy or the general form provided by Ffowcs-Williams & Hawkings, or wave extrapolations. The following discrete expression is considered:

$$4\pi p_a(\mathbf{x_i}, t_a^l) - \sum_{j}^{Ny_s} S\left(\mathbf{y}_j, t_a^l - \frac{|\mathbf{x_i}-\mathbf{y_j}|}{c_0}\right) \frac{\Delta V_{y_j}}{|\mathbf{x_i}-\mathbf{y_j}|} \tag{2}$$

where ΔV_{y_j} is the elementary volume attached to the j^{th} source element located at $\mathbf{y_j}$, and Ny_s is the number of source elements. If it is assumed that Nt_s datafiles of the source term S can be computed and sampled at Δt_s, one have to interpolate the source quantity at the time $t_a - \frac{|\mathbf{x_i}-\mathbf{y_j}|}{c_0}$ in order to compute the acoustic quantity on given $\mathbf{x}$ and t_a grids.

One key point is how to organise the loops on the source elements, source fields, and in the present case, observer points. The most straightforward procedure consists in fixing the observer time and location, and collecting the contribution of each source point in the datafiles which bound the retarded-time. The advanced time principle (Casalino [4], Kessler & Wagner [5]) consists in fixing the source time first, and then radiating the contribution at the observer points at a reception time which is determined by the source-observer distance. The present algorithm is dedicated to configurations for which the source-observer distances cannot be stored in a local variable. This happens when a $2D$ acoustic field is computed (not only a signal at a couple of observer points) using $3D$ or large $2D$ source grids (e. g. volumic source distributions).

Let l be fixed such as $t_a^l = l\Delta t_s$, thus defining the reception time when the acoustic picture is to be computed. Following the advanced time principle, let be fixed a source time interval, bounded by $k\Delta t_s$ and $(k+1)\Delta t_s$, where the source quantity is available. Consequently, the [source-observer] pairs involved at this step of the accumulation process are such that:

$$(l-(k+1))c_0\Delta t_s < r_{ij} \leq (l-k)c_0\Delta t_s \tag{3}$$

where $r_{ij} = |\mathbf{x_i} - \mathbf{y_j}|$. Thus, if the source point j is also fixed, its contribution radiates at observer points located within a circular stripe, ring, centered on him between the radii $r_1 = (l-(k+1))c_0\Delta t_s$ and $r_2 = (l-k)c_0\Delta t_s$. So it is necessary to cover this set of observer points.

One method is to scan the whole observer grid, and test the distance condition (3). This method leads to the computation of all the $Ny_s \times Nx_o$ distances at each time step, where Nx_o is the number of observer point, and the CPU-time of the acoustic prediction is mainly spent for that. Tests simulations are performed in which the extent of the source and observer domains are fixed ; consequently, the number of time steps $Nt_s = 755$ is fixed too. The results for this method are shown in figure 1-left for 6 combinations of the source and observer grids. The resulting linear regression function is:

$$T_{SCAN} \propto 3,4.10^{-10} \times Nt_s \times Nx_o \times Ny_s \tag{4}$$

where T_{SCAN} is the CPU-time in minutes of a simulation using the scanning emission time algorithm.

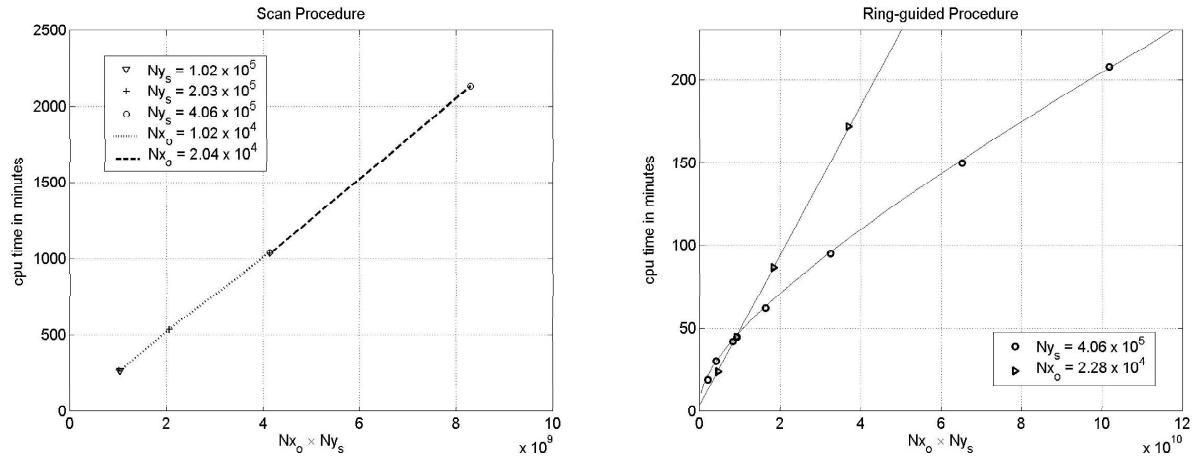

Figure 1. CPU-time of test simulations with respect to the number of source-observer pairs, for different grid combination. Left: scanning emission-time procedure; right: ring-guided emission-time procedure (solid line from estimation (5).)

B. An optimized algorithm

The optimised method developed here consists in covering the set of observer points defined by (3) without having the source-observer distances stored nor computing all of them at each time step: split a rectangular shaped acoustic field with a uniform grid, in 4 arcs with right angles from the main directions; then, e. g. for the top right arc, start vertically above the source point and outside the ring (*suburbs*), move down testing the source observer distance ; once the *intramural district* is reached, move right to the next observer vertical line and start again from outside. This behaves like a recursive marching, and by avoiding numerous source-observer distance computations, it is much less consuming than the scanning algorithm, as visible in figure 1-right. For example, the ratio is 35 for the case $Ny_s = 4,06.10^5$ and $Nx_o = 1,02.10^4$, and the ratio is 50 for the case $Ny_s = 4,06.10^5$ and $Nx_o = 2,04.10^4$. The ring-guided algorithm has also a different behavior with respect to the observer grid, however it is still proportional to the number of source points Ny_s. The key parameter is $\Delta x_o/(c_0\Delta t_s)$, where Δx_o is the observer grid step. If it is low, there are statistically many observer points found on the ring with respect to the number of points tested, since the ring thickness is $(c_0\Delta t_s)$. Thus, the effiency is increased. It is obtained that:

$$T_{RING} \propto \left(1,02\frac{\Delta x_o}{c_0\Delta t_s} + 0,92\right).10^{-9} \times Nx_o \times Ny_s \tag{5}$$

where T_{RING} is the CPU-time in minutes of a present simulation using the ring-guided procedure. Unlike T_{SCAN}, T_{RING} does not depend explicitely on Nt_s because it is linked to the total number of integration operation, which is always $Nx_o \times Ny_s$.

III. Validation of the procedure

The simulations which leaded to the cost estimation of the previous section were performed for a two-dimensional source domain, located in the same plane as the observer domain. The same behavior is expected for a source plane which would not be placed in the same plane as the observer grid. However, in that case, the condition (3) has to be projected in the observer plane. Moreover, the solution (1) is obtained using the three-dimensional Green function. Consequently, a two-dimensional source will not give the physically correct acoustic field which is the solution of the full 2D problem formulation. In order to provide a general methodology, it is thus necessary to write the algorithm for the spanwise direction.

A. Implementation in the spanwise direction

Let fix again the reception time and the source time interval. Source-observer pairs involved are such that :

$$(l-(k+1))c_0\Delta t_s < r_{ij} \leq (l-k)c_0\Delta t_s \tag{6}$$

where the reception time is defined by $t_a^l = l\Delta t_s$, the source fields are known at $k\Delta t_s$ and $(k+1)\Delta t_s$, and $r_{ij} = |\mathbf{x_i} - \mathbf{y_j}|$. If the source location is fixed as well, (6) defines two spheres centred on it of radii $r_1 = (l-(k+1))c_0\Delta t_s$ and $r_2 = (l-k)c_0\Delta t_s$. Thus, in the observer plane, defined by $y_3 = 0$, observer points verifying (6) are within two circles centred on $(x_1 = y_1,\ x_2 = y_2)$ of radii r_1' and r_2' defined by:

$$r_1' = \sqrt{r_1^2 - y_3^2} \quad \text{and} \quad r_2' = \sqrt{r_2^2 - y_3^2}$$

These geometric relations are sketched in figure 2.

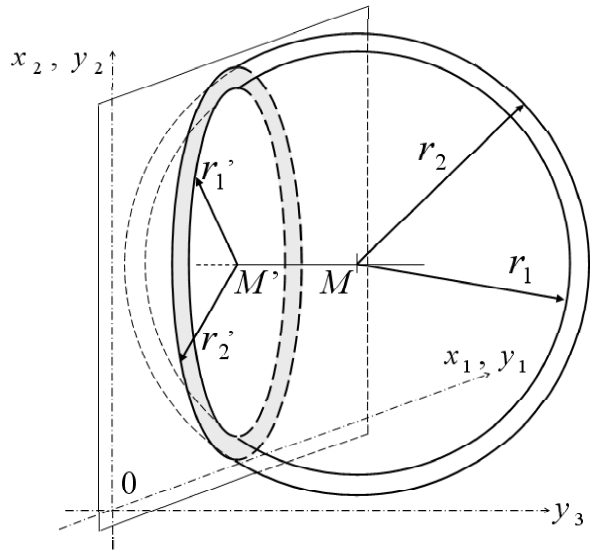

Figure 2. Sketch of the configuration for the implementation in the spanwise direction. M **is the source point, located in** (y_1, y_2, y_3) **;** (x_1, x_2) **are the coordinates in the observer plane ;** r_1 **and** r_2 **are the propagation distances defined by 3 ;** r_1' **and** r_2' **are the corresponding radii of the circles obtained where the spheres centred on the source point cut the observer plane.**

If the grid in the spanwise direction is basically an extrusion of the grid in the $(\mathbf{y_1}, \mathbf{y_2})$ plane, the procedure is the following:

1. fix (loop on) the source field(s)
2. fix (possibly loop on) the reception time(s); the propagation distances r_1 and r_2 are computed.
3. fix (loop on) the source location(s) in the spanwise direction; the radii r_1' and r_2' in the observer plane are computed.
4. fix (loop on) the source coordinates $(y_1,\ y_2)$, search the observer points located within the two circles, and add the interpolated source contribution to the acoustic pressure at them.

Appropriate tests can be introduced at the third step in order to restrict the loop to spanwise source locations which effectively radiate in the observer plane at this time step. If y_3 is too far, the propagation distance may be too short and the emission may not reach the observer plane. If y_3 is too small, the propagation distance may be too large and involve observer locations outside the desired observer grid.

The search procedure at the fourth step is performed using the same methodology as in the previous section: splitting the ring in 4 arcs, and for each grid step in the $\mathbf{x_1}$ direction, finding the grid steps in the $\mathbf{x_2}$ direction satisfying (6). As sketched in figure 3, for a given step i_1 such as $x_1 = (i_1 - 1)\Delta x_1$, the observer points located on the ring are at indices i_2 such as:

$$\sqrt{(r_1')^2 + (x_1 - y_1)^2} < (i_2 - 1)\Delta x_2 \leq \sqrt{(r_2')^2 + (x_1 - y_1)^2} \tag{7}$$

So a loop on the second observer coordinate can be introduced, bounded by $i_2^{(1)}$ and $i_2^{(2)}$ given by:

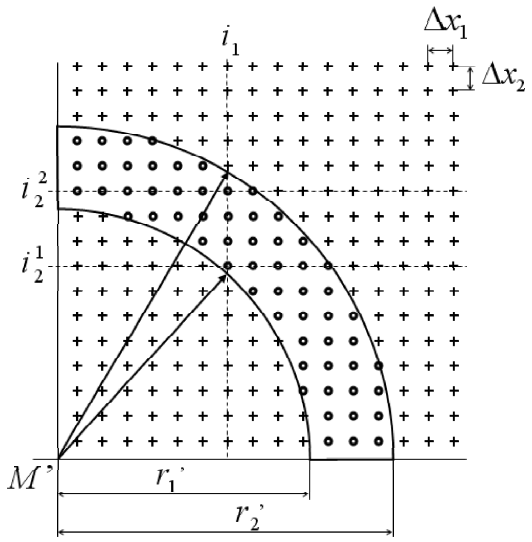

Figure 3. Principle of the extraction of the observer points located on the ring. M', r_1' and r_2' are defined in figure 2; Δx_1 and Δx_2 are the grid steps in the observer plane.

$$i_2^{(1)} = int\left[\frac{\sqrt{(r_1')^2 + (x_1 - y_1)^2}}{\Delta x_2}\right] + 2 \quad \text{and} \quad i_2^{(2)} = int\left[\frac{\sqrt{(r_2')^2 + (x_1 - y_1)^2}}{\Delta x_2}\right] + 1$$

B. Test-case: monopole source

The implementation of the procedure is validated through the case of a harmonic source located at the origin in a two-dimensional configuration. The source quantity to integrate in (1) is defined as:

$$S(\mathbf{y}, \tau) = \delta(\mathbf{y})\ A\ d\sigma\ \sin(\omega\ \tau) \tag{8}$$

where δ is the Dirac function, A is the source amplitude, $d\sigma$ the elementary surface over which it extends and ω is the angular frequency.

1. The 2D Green function

In the time domain, the 2D Green function is given by:[6]

$$G_{2D}(\mathbf{x}, t|\mathbf{y}, \tau) = -\frac{H\left(t - \tau - r/c_0\right)}{2\pi\sqrt{c_0^2(t-\tau)^2 - r^2}} \tag{9}$$

where H is the Heavyside function and $r = |\mathbf{x} - \mathbf{y}| = \sqrt{(x_1 - y_1)^2 + (x_2 - y_2)^2}$. Thus the general solution of the inhomogeneous wave equation is:

$$p(x_1, x_2, t) = -\frac{1}{2\pi}\int_{-\infty}^{+\infty}\int_{-\infty}^{+\infty}\left(\int_{-\infty}^{+\infty}\frac{H\left(t - \tau - r/c_0\right)}{\sqrt{(t-\tau)^2 - r^2/c_0^2}} S\left(y_1, y_2, \tau\right) d\tau\right) dy_1 dy_2 \tag{10}$$

Integrating the Heavyside function,[7] it yields:

$$p(x_1, x_2, t) = -\frac{1}{2\pi}\int_{-\infty}^{+\infty}\int_{-\infty}^{+\infty}\left(\int_{-\infty}^{t - r/c_0}\frac{S\left(y_1, y_2, \tau\right)}{\sqrt{(t-\tau)^2 - r^2/c_0^2}} d\tau\right) dy_1 dy_2 \tag{11}$$

It is relatively straightforward to convert the time integral into an integration over a third spatial direction, noted y_3. One obtains:

$$p(x_1,x_2,0,t)=\frac{1}{2\pi}\int_{-\infty}^{+\infty}\int_{-\infty}^{+\infty}\left(\int_{-\infty}^{0}\frac{S\left(y_1,y_2,0,t-\frac{\sqrt{r^2+y_3^2}}{c_0}\right)}{\sqrt{r^2+y_3^2}}dy_3\right)dy_1dy_2 \tag{12}$$

This formulation shows how the procedure developed here can be validated or applied in a 2D configuration, provided that a 3D Green function is combined with a space integration over the spanwise direction and a replication of the source data known in the (y_1, y_2) plane.

2. Reference solution

The acoustic field of the source defined by (8) is thus given by:

$$p(x_1,x_2,t)=\frac{Ad\sigma}{2\pi}\int_0^{\infty}\frac{\sin\left[\omega(t-\frac{\sqrt{x_1^2+x_2^2+y_3^2}}{c_0})\right]}{\sqrt{x_1^2+x_2^2+y_3^2}}dy_3 \tag{13}$$

Preliminary tests have shown that at least 200 wavelenthes were necessary in the spanwise direction to obtain less than 1% of error on the value of the integral. Such bound depends on the grid step in this direction, noted Δy_3, but using the trapezoid rule, no improvement of the precision is observed for steps smaller than one eighth of the wavelength.

The acoustic pressure computed with the algorithm presented in sections II and A is compared to the reference solution obtained by computing directly (13). This allows to valid the implementation of the various loops, of the interpolation and of the integration operation. As plotted in figure 4 for $\omega = 2\pi$, $A = 1$, $d\sigma = 1$, $c_0 = 1$ and $t = 10\pi/\omega$, an excellent agreement is found. 30 points by period were used to discretize the source signal, and the interpolation is linear. A better precision can be achieved in far field using a finer time resolution of the source signal.

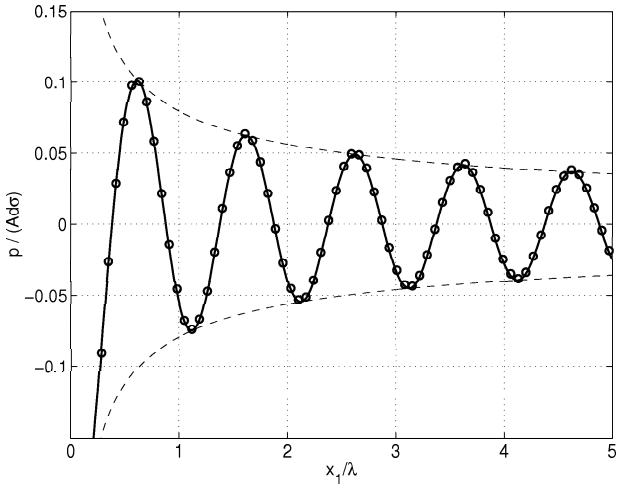

Figure 4. Acoustic pressure field for a monopole source in 2D. Straight line: reference solution; Symbols: algorithm solution; dashed line: $r^{-0.5}$ laws.

IV. Extension to convection effects

A. The convected Green function

For the propagation in a uniformly moving flow at the subsonic Mach number M_0 in the direction $\mathbf{y_1}$, the 3D convected Green function in the time domain is given by:[8]

$$\tilde{G}_{2D}(\mathbf{x},t|\mathbf{y},\tau)=-\frac{\delta\left(t-\tau+\tau^*\right)}{4\pi\, r_\beta} \tag{14}$$

where $\beta^2 = 1 - M_0^2$, $r_\beta = \sqrt{(x_1-y_1)^2 + \beta^2\left[(x_2-y_2)^2 + (x_3-y_3)^2\right]}$ and $\tau^* = \dfrac{r_\beta - M_0(x_1-y_1)}{c_0\beta^2}$

The integral solution for the acoustic pressure is thus given by:

$$p_a(\mathbf{x},t_a) = \frac{1}{4\pi}\int_{\mathcal{D}} S\left(\mathbf{y}, t_a - \frac{r_\beta - M_0(x_1-y_1)}{c_0\beta^2}\right)\frac{d\mathbf{y}}{r_\beta} \tag{15}$$

B. Adaptation of the algorithm

According to the present methodology, one have to fix the reception time t and a pair of emission times τ and $\tau + d\tau$. Then one have to find the source-observer pairs for which the propagation time τ^* satisfies:

$$t - (\tau + d\tau) < \tau^* < t - \tau \tag{16}$$

that is

$$(l - (k+1))c_0\Delta t_s < \frac{r_\beta - M_0(x_1-y_1)}{\beta^2} \leq (l-k)c_0\Delta t_s \tag{17}$$

It is relatively straigthforward to show that for a fixed $\mathbf{y}$, the following equation:

$$\sqrt{(x_1-y_1)^2 + \beta^2\left[(x_2-y_2)^2 + (x_3-y_3)^2\right]} - M_0(x_1-y_1) = R\beta^2 \tag{18}$$

where R is a constant, is the equation of a sphere centred on $(y_1 + RM_0, y_2, y_3)$ of radius R. Consequently, the algorithm presented in section III A can be applied using the convected Green function, provided that the centre of the circles are moved downstream the source point by the distance RM_0, and that $|\mathbf{x}-\mathbf{y}|$ is replaced by r_β at the denominator in the integration. However, the two circles have not the same centre, and the centre location depends on the current propagation time. These two trends are more marked when the Mach number increases. The solution for a fixed observer domain is recovered when making $M_0 = 0$.

The acoustic pressure computed with the algorithm adapted to the convected propagation case is compared to the reference solution obtained by computing directly (15). As plotted in figure 5 for $\omega = 2\pi$, $A = 1$, $d\sigma = 1$, $c_0 = 1$, $t = 8\pi/\omega$, and $M_0 = 0.5$, an excellent agreement is found. The propagation in a moving flow leads to a different wavelength between observers located upstream and observers located downstream.

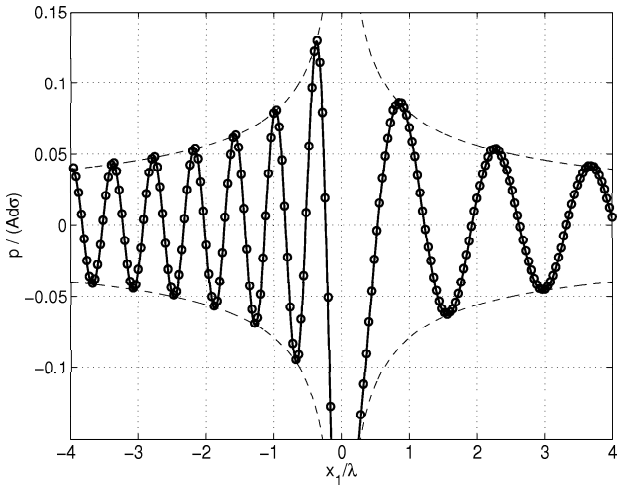

Figure 5. Acoustic pressure field for a monopole source in 2D, with convection effects. Straight line: reference solution; Symbols: algorithm solution; dashed line: $r^{-0.5}$ laws.

In figure 6, the acoustic field of the same monopole as in section III B but radiating in an uniform flow is plotted for different Mach numbers of this flow.

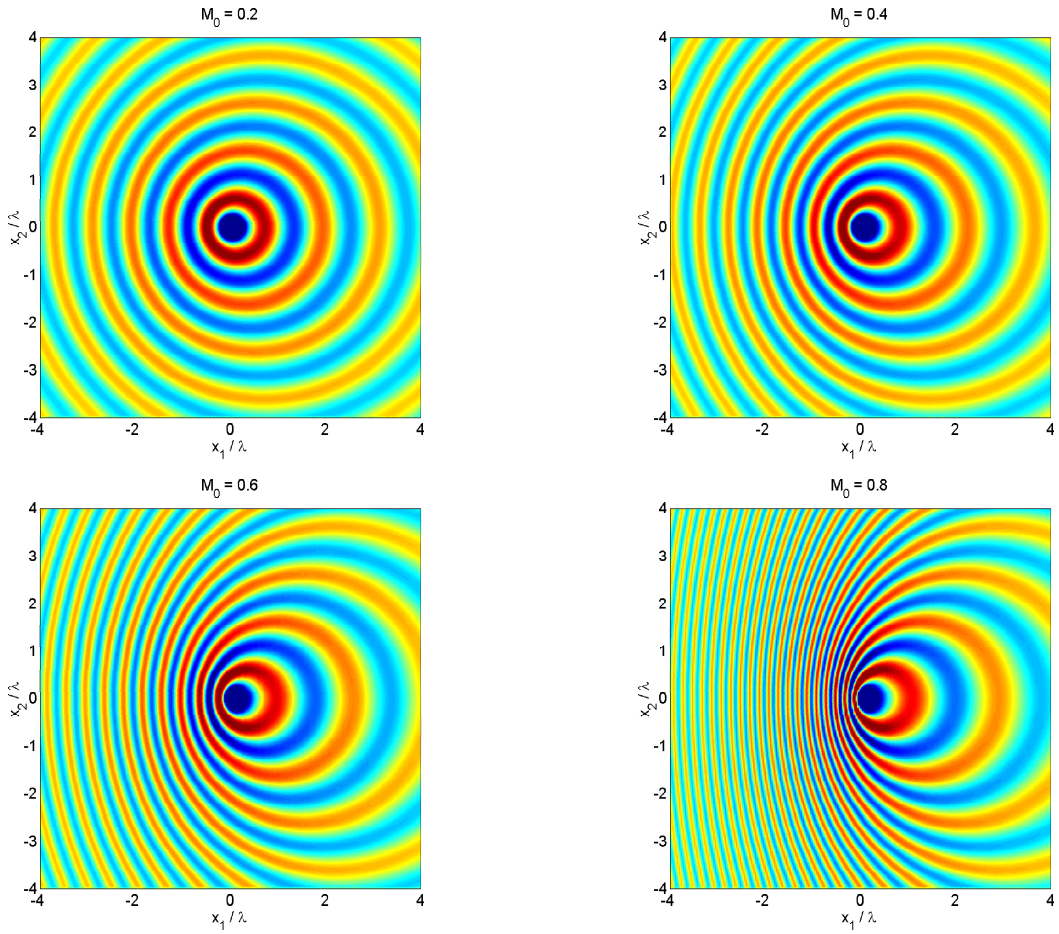

Figure 6. Acoustic pressure field of a harmonic source of unit amplitude placed in a uniform flow, for different Mach numbers of this flow. Levels are from -0.1 **to** 0.1

V. Application to the aeolian tone prediction

Finally, the present methodology is applied to the aeolian tone prediction. This is a test-case with several source points and with real flow source data. Thus, it illustrates well the practical configuration adressed by the present algorithm development. In this flow case, the main source quantity is the pressure fluctuation at the cylinder wall, as written in Curle's analogy.[9] The source data is provided by a two-dimensional numerical simulation using a tool similar to the one presented by Gloerfelt *et al.*[10] The flow is at the Mach number $M_0 = 0.3$ and the Reynolds number $Re = 136$. At these conditions, a periodic vortex shedding state is achieved. Two hundred source fields are saved by period.

The reference computation is performed in the Fourier domain, using the 2D spectral convected Green function. The spatial derivatives appearing in Curle's analogy are perfomed on the Green function itself, thus providing an exact formulation. For the computation in the time domain, the spanwise extent is about $1000a$, where a is the cylinder radius, which corresponds to approximately 30 wavelenthes. The spanwise direction step is $\Delta y_3 = 2.5a$, what provides about 15 points by wavelenth. The spatial derivatives are performed in post-treatment, using an fourth-order explicit finite difference scheme.

Validation is first provided without convection effect. The acoustic pressure generated along the x_2 axis by lift fluctuations is represented in figure 7, and show a very good agreement between the two computation methods. In the vicinity of the cylinder, the acoustic field becomes singular, since the upper and lower sides are out of phase. Consequently, the space derivation leads to unphysical results in that region for the temporal computation using a relatively coarse observer grid.

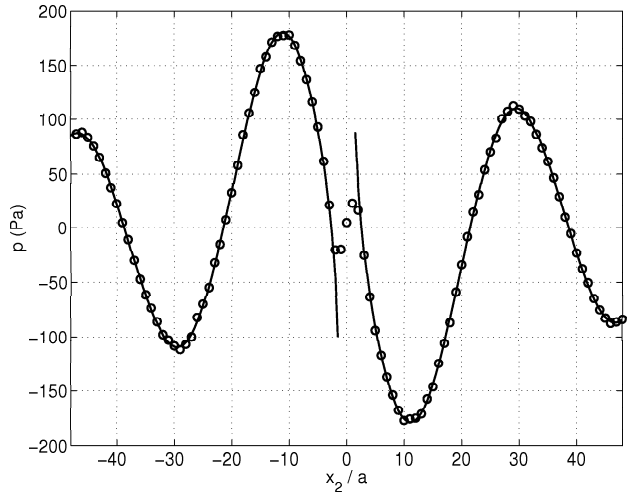

Figure 7. Acoustic pressure field generated by lift fluctuations on a cylinder with no convection effect included in the propagation. Straight line: reference solution; Symbols: algorithm solution.

Finally, the convected case shows the good behavior of the present algorithm in a practical case. The acoustic pressure field generated by lift fluctuations is plotted in figure 8. The directivity is modified by convection effects, and this is well tracked by both methods. Some minor oscillations are visible on the field computed in the time domain, which may be attributed for some part to the space derivation over the observer grid. Also, the source data are not exactly periodic, what leads to a spurious noise in the computation in the time domain. Indeed, such noise is avoided in the computation in frequency domain by removing the highest modes from the source spectrum.

VI. Concluding remarks

An optimized method has been developed for the computation of retarded-time integrals. The present optimization concerns the evaluation of the acoustic field on an observer grid, thus involving a large number of source-observer distances which can not be stored in a local variable. An iterative ring-guided procedure is proposed which recursively searches observer points where the contribution of a given source point must be added once both the emission and reception time are fixed. Such a procedure appeared very faster than an intuitive search method in that context. It can

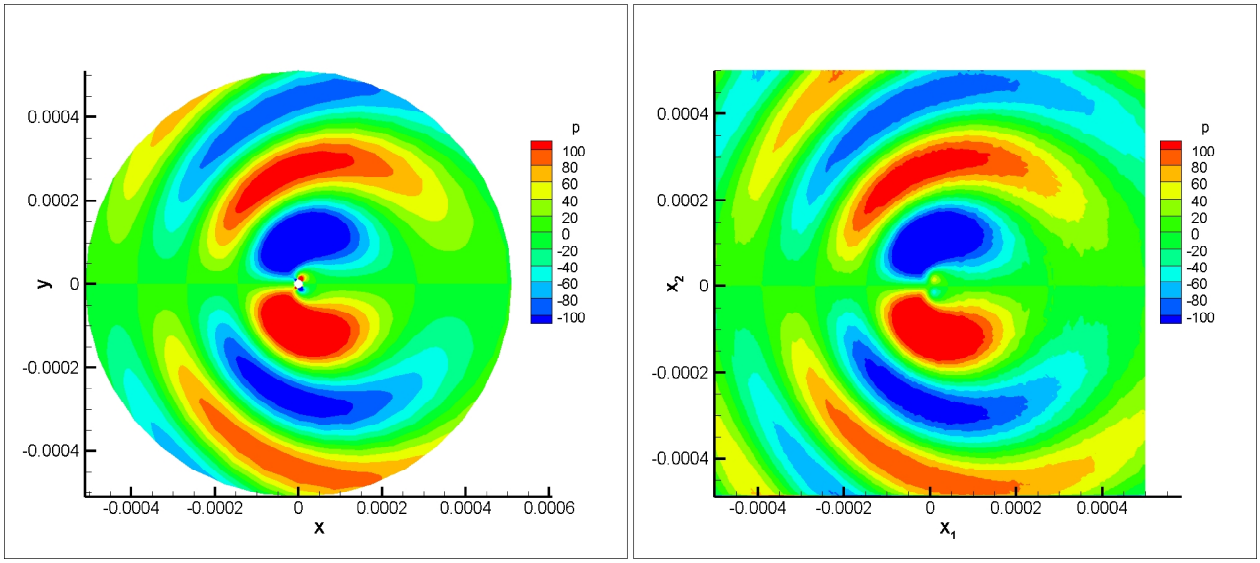

Figure 8. Acoustic pressure field generated by lift fluctuation on a cylinder in a 2D uniform flow at Mach number $= 0.3$. Left: computation with the spectral convected Green function; right: computation with the temporal convected Green function using the present algorithm.

be used for all kinds of retarded-time integrals, such as volume sources in Lighthill-like formalisms as well as surface sources in Kirchhoff-like wave extrapolation methods. It keeps the advanced time principle allowing an acoustic prediction parallel to the flow simulation and an easy connection with usual CFD tools. The observer grid step has no influence on the precision of the computed acoustic pressure, since there is no relation between the observer points (through numerical schemes, for instance). However, the observer grid affects the global CPU-time and the efficiency of the algorithm, and determines the resolution of the output image. Finally, it is worth noting that using the present methodology, there is no additional cost using a 3D source domain, in relation to a 2D problem.

Acknowledgments

The author gratefully acknowledge X. Gloerfelt for sharing source data and reference solution for the cylinder flow.

References

[1]T. Colonius, and S. K. Lele, “Computational aeroacoustics: progress on nonlinear problems of sound generation”, Prog. Aerospace Sc., 40, 345-416 (2004).

[2]M. Wang, J. B. Freund and S. K. Lele, “Computational prediction of flow-generated sound”, Ann. Rev. Fluid Mech., 38, 483-513 (2006).

[3]M. J. Lighthill, “On sound generated aerodynamically. I. General theory”, Proc. Roy. Soc. A, Vol. 223, pp. 1-32, (1952).

[4]D. Casalino, “An advanced time approach for acoustic analogy predictions”, J. Sound Vib., 261(4),583-612 (2003).

[5]M. Kessler, and S. Wagner, ”Source-time dominant aeroacoustics”, Comp. Fluids, 33, 791-800 (2004).

[6]D. G. Crighton, A. P. Dowling, J. E. Ffowcs Williams, M. Heckl and F. G. Leppington, ” Modern methods in analytical acoustics : Lectures notes”, Springer Verlag, London, (1992).

[7]I. M. Guelfand and G. E. Chilov, ”Les Distributions”, Dunod, Paris, (1962).

[8]Howe M. S., ”Acoustics of fluid-structure interactions”, Cambridge University Press, (1998).

[9]N. Curle, ”The influence of solid boundaries upon aerodynamic sound”, Proc. Royal Soc. A, 231,505-514, (1955).

[10]Gloerfelt X., Bailly C. and D. Juvé, ”Direct computation of the noise radiated bya subsonic cavity flow and application of integral methods”, Journal of Sound and Vibration, 266, 119146, (2003).